remote sensing

MDPI

Article

Spatial and Temporal Variability of Key Bio-Temperature Indicators and Their Effects on Vegetation Dynamics in the Great Lakes Region of Central Asia

Xuan Gao [1,2] and Dongsheng Zhao [1,*]

[1] Key Laboratory of Land Surface Pattern and Simulation, Institute of Geographic Sciences and Natural Resources Research, Chinese Academy of Sciences, No. 11A, Datun Road, Chaoyang District, Beijing 100101, China; gaox.19b@igsnrr.ac.cn

[2] University of Chinese Academy of Sciences, No. 19A, Yuquan Road, Shijingshan District, Beijing 100049, China

* Correspondence: zhaods@igsnrr.ac.cn; Tel.: +86-10-6488-9692

Abstract: Dryland ecosystems are fragile to climate change due to harsh environmental conditions. Climate change affects vegetation growth primarily by altering some key bio-temperature thresholds. Key bio-temperatures are closely related to vegetation growth, and slight changes could produce substantial effects on ecosystem structure and function. Therefore, this study selected the number of days with daily mean temperature above 0 °C (DT_0), 5 °C (DT_5), 10 °C (DT_{10}), 20 °C (DT_{20}), the start of growing season (SGS), the end of growing season (EGS), and the length of growing season (LGS) as bio-temperature indicators to analyze the response of vegetation dynamics to climate change in the Great Lakes Region of Central Asia (GLRCA) for the period 1982–2014. On the regional scale, DT_0, DT_5, DT_{10}, and DT_{20} exhibited an overall increasing trend. Spatially, most of the study area showed that the negative correlation between DT_0, DT_5, DT_{10}, DT_{20} with the annual Normalized Difference Vegetation Index (NDVI) increased with increasing bio-temperature thresholds. In particular, more than 88.3% of the study area showed a negative correlation between annual NDVI and DT_{20}, as increased DT_{20} exacerbated ecosystem drought. Moreover, SGS exhibited a significantly advanced trend at a rate of −0.261 days/year for the regional scale, while EGS experienced a significantly delayed trend at a rate of 0.164 days/year. Because of changes in SGS and EGS, LGS across the GLRCA was extended at a rate of 0.425 days/year, which was mainly attributed to advanced SGS. In addition, our study revealed that about 53.6% of the study area showed a negative correlation between annual NDVI and LGS, especially in the north, indicating a negative effect of climate warming on vegetation growth in the drylands. Overall, the results of this study will help predict the response of vegetation to future climate change in the GLRCA, and support decision-making for implementing effective ecosystem management in arid and semi-arid regions.

Keywords: climate change; normalized difference vegetation index; bio-temperature; Great Lakes Region of Central Asia

Citation: Gao, X.; Zhao, D. Spatial and Temporal Variability of Key Bio-Temperature Indicators and Their Effects on Vegetation Dynamics in the Great Lakes Region of Central Asia. *Remote Sens.* **2022**, *14*, 2948. https://doi.org/10.3390/rs14122948

Academic Editors: Ayyoob Sharifi, Baojie He, Chi Feng and Jun Yang

Received: 28 April 2022
Accepted: 16 June 2022
Published: 20 June 2022

1. Introduction

Global surface temperature was 1.09 °C higher in 2011–2020 than 1850–1900, with larger increases over land (1.59 °C) than over the ocean (0.88 °C) [1]. Climate change characterized by global warming has a greater impact on the structure and function of terrestrial ecosystems [2,3]. Climate warming has intensified glacier melting and permafrost degradation [4,5], resulting in a series of ecological and environmental effects, such as the release of large amounts of deep permafrost carbon and the declining water table [6]. Meanwhile, climate warming enhanced vegetation productivity by promoting photosynthesis, extending growing seasons, especially at high latitudes and altitudes [7–9]. In addition, plenty of evidence suggests that extreme high-temperature events are increased with enhancement

of frequency and intensity across the globe [10,11]. Although climate warming reduces the occurrence of extremely low temperature events, such as frost events, the extension of the plant growing season due to warming may induce more frequent frost days during the growing season [12,13]. Accompanied by changes in temperature, the adaptive capacity of vegetation to environmental changes and ecosystem vulnerability increases, significantly affecting the provision of global ecosystem services [14]. Therefore, monitoring vegetation growth and understanding its response to temperature change is important for quantifying global carbon budget, and has become a hot topic in climate change research [15,16].

Ecosystems in arid and semi-arid regions are more fragile to climate change due to harsh environmental conditions, and even slight changes in the climate can have a substantial influence on such ecosystems [17,18]. However, previous studies on climate change have mainly focused on the analysis of statistical distributions of climate variables, such as mean, maximum, and minimum values, while neglecting their association with ecosystems [19,20]. Climate change affects vegetation growth primarily by altering some key bio-temperature thresholds, such as 0 °C, 5 °C, 10 °C, and 20 °C [21–23]. These temperature indicators are closely related to the growth and distribution of vegetation, and their changes may lead to alterations in ecosystem structure and function [24–26]. Recent evidence has indicated that changes in bio-temperature thresholds altered vegetation productivity and modified vegetation seasonality by affecting the initiation, termination, and performance of vegetation photosynthetic activity over the Northern Hemisphere land [27]. Meanwhile, the Normalized Difference Vegetation Index (NDVI), as a typical remote sensing index for measuring vegetation greenness, was widely used to characterize the response of vegetation growth to climate change [7,19,28]. In recent decades, numerous studies have indicated that variations in global temperature have greatly affected vegetation dynamics in drylands [29,30]. Nevertheless, few studies were focused on the relationship between key bio-temperature thresholds and NDVI. A quantitative assessment of the effects of changes in key bio-temperature thresholds on NDVI will be helpful for understanding the response mechanisms of dryland ecosystems to climate change.

The Great Lakes Region of Central Asia (GLRCA) is located in the hinterland of the Eurasian continent, far from the ocean, and covers five countries: Kazakhstan, Kyrgyzstan, Turkmenistan, Tajikistan, and Uzbekistan, which is the largest dryland area in the temperate zone of the Northern Hemisphere [31,32]. Over the past 33 years, the GLRCA has experienced rapid warming of approximately 0.36 °C–0.42 °C, which was stronger than the global average temperature [33]. Greater warming significantly affects the intensity and frequency of extreme temperatures in the GLRCA, with an overall trend of increased extreme high-temperature events and decreased extreme low-temperature [29,34,35]. Arid and semi-arid regions are very sensitive to climate change due to their fragile ecosystems and limited resilience to climate change [36]. Temperature changes can be directly reflected in changes in vegetation growth [29,37]. Zhou et al. [38] found that the warming trend in the GLRCA initially enhanced the greenness of vegetation before 1991, but then the continued warming trend inhibited further increase in greenness. In addition, several studies have also demonstrated that the increase in temperature prolonged the growing season, and in turn increased ecosystem productivity in some areas of the GLRCA [37,39]. However, it remained uncertain how key bio-temperature thresholds changed over the GLRCA, and different bio-temperature may induce various impacts on terrestrial ecosystems under global warming. Therefore, it is essential to explore the spatial and temporal associations of vegetation growth and key bio-temperature thresholds in the GLRCA.

In this study, we selected the number of days with daily mean temperature above 0 °C (DT_0), 5 °C (DT_5), 10 °C (DT_{10}), 20 °C (DT_{20}), the start of growing season (SGS), the end of growing season (EGS), and the length of growing season (LGS) as key indicators of bioclimatology. Based on these indicators, the objectives of this study were to (1) investigate the temporal and spatial trends of bio-temperature in the GLRCA; and (2) explore the correlation between NDVI and bio-temperature indicators, thus detecting the response of vegetation growth to temperature changes. This study provides a scientific basis for

quantitative assessment of vegetation growth changes in dryland ecosystems under global warming, and will be helpful for decision-making in implementing ecological restoration and conservation in arid and semi-arid regions.

2. Data and Methods

2.1. Study Azrea

GLRCA (35.1–55.5°N, 46.4–87.4°E) includes five Central Asian countries: Kazakhstan, Uzbekistan, Turkmenistan, Kyrgyzstan, and Tajikistan [31]. The entire study area is dominated by a typical continental climate, characterized by scarce precipitation, strong evapotranspiration, and large temperature fluctuations [40]. Meanwhile, precipitation in the GLRCA is controlled by westerly and monsoon, and differences in moisture sources further influence precipitation patterns, with precipitation mainly concentrated in spring [41–43]. Different periods of rain and heat develop a more unique dryland ecosystem that is highly sensitive to climate change [44,45]. Grasslands (70.1%), barren land (16.8%), croplands (5.5%), and shrublands (3.1%) are the major land cover types in the GLRCA (Figure 1a). Additionally, GLRCA can be divided into three climate zones based on the Koppen–Geiger climate classification [46]: arid climate zone, cold climate zone, and temperate climate zone (Figure 1b). Arid climate zone and cold climate zone account for 63.0% and 36.4% of the study area, respectively.

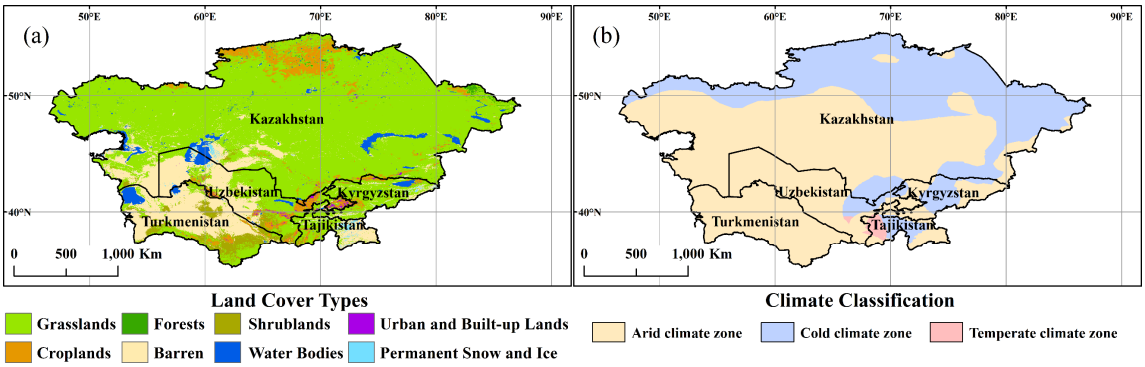

Figure 1. (**a**) The land cover types (Source: MCD12Q1, https://modis.gsfc.nasa.gov/data/, accessed on 20 September 2021), and (**b**) the climate classification in the study area.

2.2. Data

2.2.1. NDVI Data

Remote sensing data, characterized by time continuity and large spatial scales, is an efficient approach to monitoring the growth status and cover of vegetation [47], and has been widely used in vegetation response to climate change studies [37,48]. In this study, we used the Global Inventory Monitoring and Modeling Studies (GIMMS) NDVI dataset from 1982 to 2014 at a spatial resolution of 0.083° × 0.083° and a bimonthly time resolution. This dataset is corrected through a series of processing steps to reduce noise interference from volcanic eruptions and sensor-induced errors, with high quality. In this study, we used the maximum value composite (MVC) method for two NDVI images of each month to obtain the monthly NDVI dataset. MVC, which processes a series of multi-temporal georeferenced satellite data into one image by examining each value pixel by pixel, retaining only the highest value at each pixel location [7,28]. To characterize the yearly growth of vegetation, yearly NDVI was defined as the average monthly composite NDVI.

2.2.2. Climate Data

The daily mean temperature data used in this study were obtained from the GLDAS-2.0 dataset provided by the Global Land Data Assimilation System (GLDAS), covering our study period (1982–2014), with a spatial resolution of 0.25° × 0.25°. GLDAS combines simulation models with observations to provide long-term gridded meteorological datasets

on a global scale, and has been widely used in climate change research [49–51]. Ji et al. [51] compared the GLDAS dataset with the Global Historical Climatology Network (GHCN) datasets (including 13511 weather stations), and found that the daily mean temperature data of GLDAS had a fairly high accuracy. Additionally, we compared and analyzed the spatial distribution of the annual means for GLDAS temperature with that for Climatic Research Unit (CRU) temperature from 1982–2014 (Figure 2), and found that they were highly consistent, which further demonstrates the applicability of GLDAS dataset in the GLRCA [33].

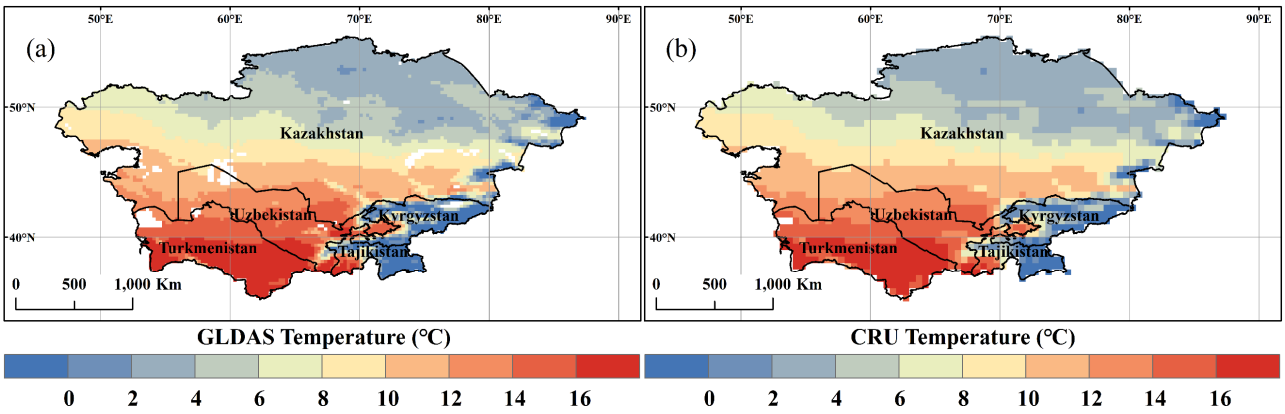

Figure 2. Spatial distribution of the annual means for (**a**) GLDAS temperature, (**b**) CRU temperature over the GLRCA from 1982–2014.

2.3. Methods

2.3.1. Bio-Temperature Indicators

Bio-temperature thresholds are closely related to the growth and distribution of vegetation, and 0 °C, 5 °C, 10 °C, 20 °C have been widely used to assess regional heat resources [21–23]. In addition, 5 °C is the minimum temperature for photosynthesis of some tropical and subtropical evergreen broadleaf forests [52]. Meanwhile, 5 °C was often employed to quantify growing season length and was also considered to be a key indicator in modelling of global vegetation patterns in previous studies [53,54]. Most thermophilic crops begin to grow when the daily mean temperature is steadily above 10 °C, and DT_{10} is closely associated with sprouting and withering of most arboreal leaves [25,55]. Furthermore, the number of days below 0 °C (frost days) and DT_{20} are commonly used to characterize the variability of extreme temperature events [26,56]. To reduce the effect of extreme values, we employed a 6-day moving average as the daily mean temperature to calculate DT_0, DT_5, DT_{10}, and DT_{20} in this study.

The effect of surface air temperature on vegetation growth is usually assessed by changes in the thermal growing season [24,57]. Considering the heat requirements for most vegetation growth, the Expert Team on Climate Change Detection and Indices (ETCCDI) defined a set of growing season indicators based on daily mean temperature, and has been widely used in climate change studies [54,58]. In the Northern Hemisphere, SGS was defined as the first day of the first 6-day period before 1 July with a daily mean temperature greater than 5 °C, and EGS was determined as the first day of the first 6-day period after 1 July with a daily mean temperature of less than 5 °C. LGS was the number of days between SGS and EGS. Ultimately, seven bio-temperature indicators were selected in this study to analyze the effect of temperature change on vegetation growth across the GLRCA (Table 1).

Table 1. The bio-temperature indicators used in this study.

Label	Index Name	Unit
DT_0	Number of days with $T_{mean} > 0$ °C	Days
DT_5	Number of days with $T_{mean} > 5$ °C	Days
DT_{10}	Number of days with $T_{mean} > 10$ °C	Days
DT_{20}	Number of days with $T_{mean} > 20$ °C	Days
SGS	Start of growing season	Julian days
EGS	End of growing season	Julian days
LGS	Length of growing season	Days

2.3.2. Correlation Analysis

To examine the response of vegetation dynamics to temperature changes, we analyzed correlations between annual NDVI and various bio-temperature indicators using Pearson's correlation coefficient based on pixels [37]:

$$r = \frac{\sum_{i=1}^{n}((x_i - \overline{x})(y_i - \overline{y}))}{\sqrt{\sum_{i=1}^{n}(x_i - \overline{x})^2 \sum_{i=1}^{n}(y_i - \overline{y})^2}} \quad (1)$$

where r is the correlation coefficient between annual NDVI and climate indicator; x_i and y_i are annual NDVI and climate data for year i, respectively; and $\overline{x}$ and $\overline{y}$ are the mean of the annual NDVI and climate data over the entire study period, respectively. An r value less (greater) than 0 indicates a negative (positive) correlation. The greater the absolute value of r, the higher the correlation between annual NDVI and bio-temperature variables.

Because of inconsistencies in the spatial resolution between the NDVI and climate data, we resampled the NDVI data from a resolution of 0.083° × 0.083° to 0.25° × 0.25° using the nearest neighbor method. Meanwhile, a p-value < 0.05 for correlation analysis was considered statistically significant.

2.3.3. Trend Analysis and Significance Test

In this study, a linear regression, calculated by the least-squares method, was performed to detect trends in NDVI and climate variables. A positive slope indicates an increasing trend and a negative slope indicates a decreasing trend. The significance of the trend was tested using the F test, and a p-value < 0.05 was considered significant. In addition, the uncertainty of the trend was defined as the difference between the slope estimates and the lower limit of the 95% confidence interval.

3. Results

3.1. Spatial and Temporal Variation of Temperature and NDVI

Figure 3 illustrates the spatial patterns of trends in annual mean temperature, annual NDVI, and correlation between annual mean temperature and annual NDVI over the GLRCA for the period 1982–2014. During the entire study period, annual mean temperature exhibited an obvious increasing trend and had large spatial heterogeneity. Greater warming (>0.050 °C/year) occurred mainly in the west and southeast. Meanwhile, approximately 68.2% of study area experienced a decreasing trend in annual NDVI. Spatially, the greater decrease (<−0.0008 year^{-1}) in annual NDVI was observed mainly in the west dominated by arid climate zone, and the greater increase (>0.0008 year^{-1}) was primarily in the east dominated by cold climate zone. To investigate the response of vegetation growth to temperature changes, we further analyzed the correlation between annual mean temperature and annual NDVI based on Pearson's correlation coefficient. From 1982 to 2014, approximately 44.0% of the study area was subject to a positive correlation between annual temperature and annual NDVI, and a greater positive correlation (>0.2) was observed primarily at high altitudes in the southeast.

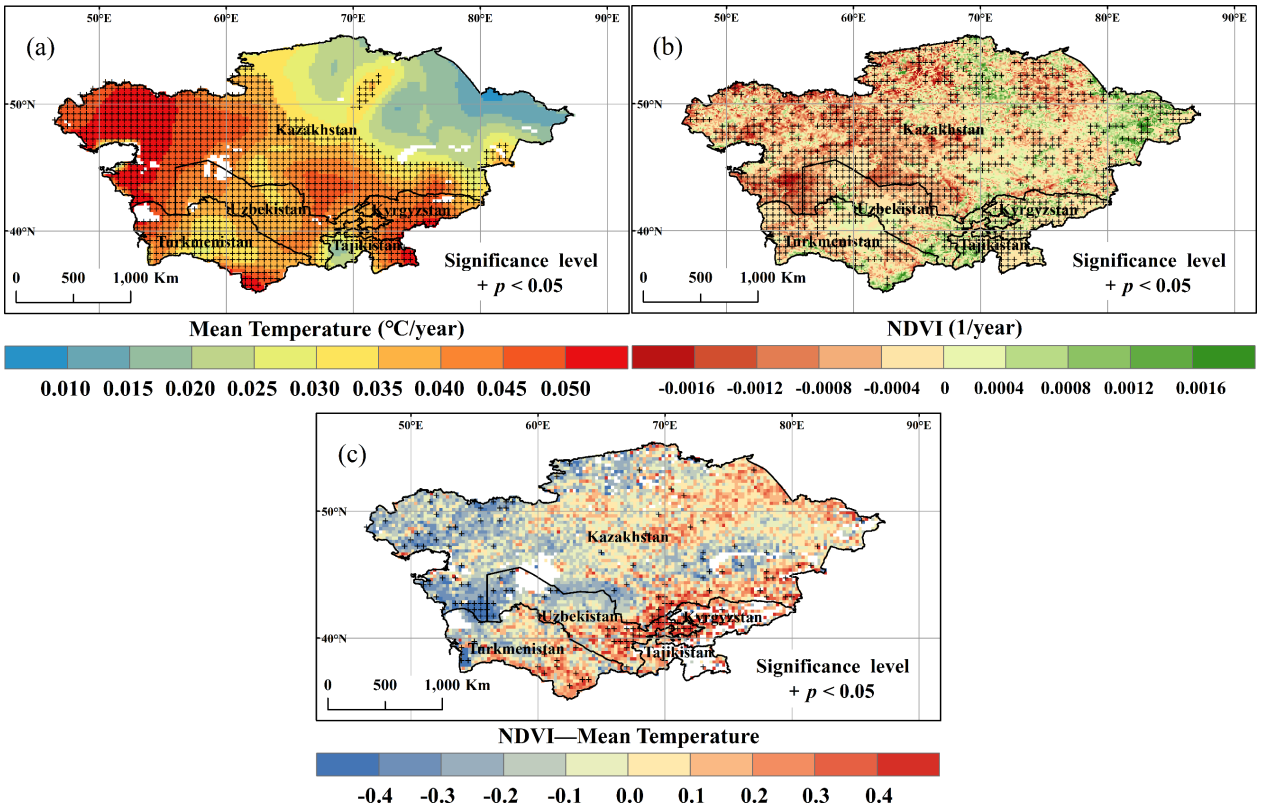

Figure 3. Spatial distribution of trends in (**a**) annual mean temperature, (**b**) annual NDVI, and (**c**) correlation between annual mean temperature and annual NDVI over the GLRCA from 1982–2014.

We employed a 6-day moving average as the daily mean temperature and then analyzed the interannual variations of maximum temperature in the GLRCA (Figure 4). From 1982 to 2014, annual means for maximum temperature in approximately 92.7% of the study area was larger than 20 °C. Relatively small annual means for maximum temperature (<20 °C) was mainly observed in the southeast with high altitudes. Overall, maximum temperature in the arid climate zone was significantly higher than in the cold climate zone. Additionally, about 70.4% of the study area was subject to an increasing trend in maximum temperature, with only 10.5% being significant ($p < 0.05$). Spatially, a larger increasing trend (>0.04 °C/year) was mainly occurred in the west of the study area dominated by arid climate zone. Interestingly, although annual mean temperature exhibited a significant increasing trend (Figure 3), the maximum temperature in 29.6% of the study area showed a decreasing trend. Greater decrease (<0.03 °C/year) was observed mostly in the northeast. Additionally, the higher uncertainty (>0.6) in the trend of maximum temperature was mainly distributed in the northwest of the study area.

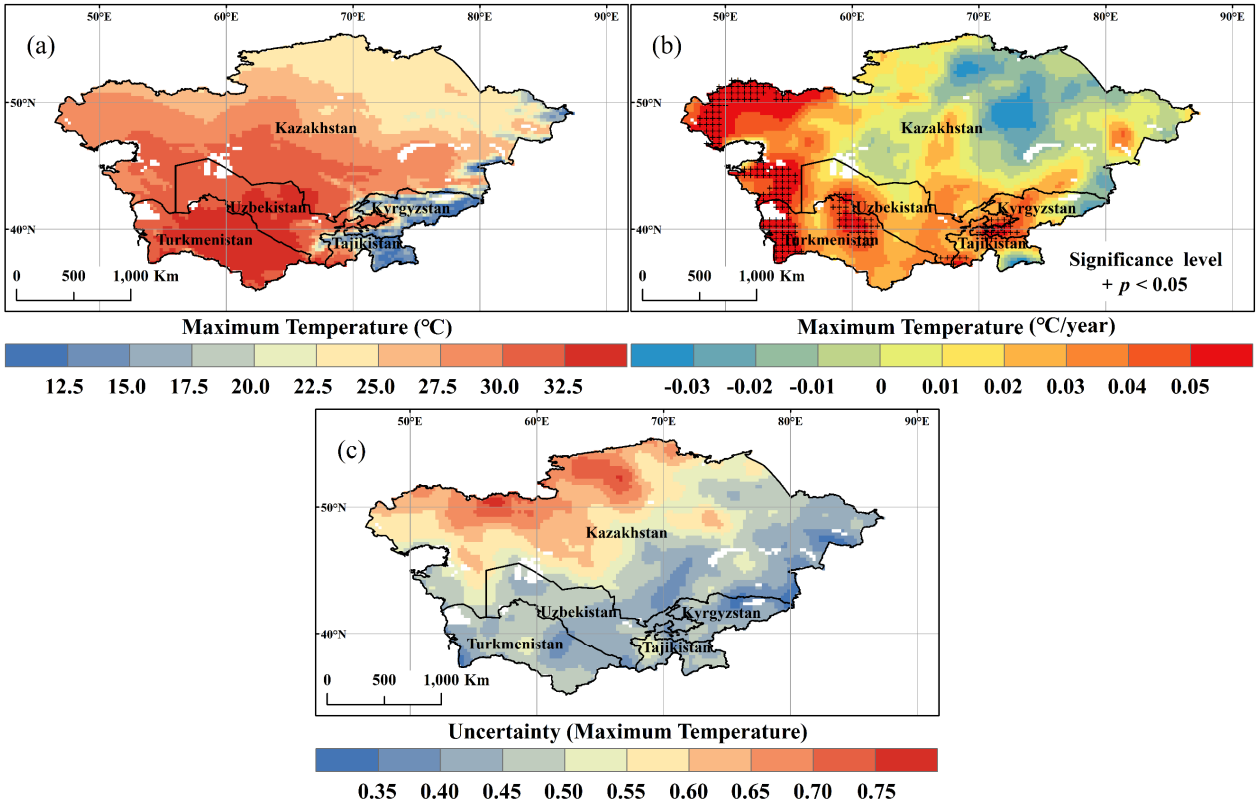

Figure 4. Spatial distribution of (**a**) the annual means for maximum temperature, (**b**) the trend for maximum temperature, and (**c**) the uncertainty in the trend of maximum temperature in the study area from 1982–2014.

3.2. Spatial and Temporal Variation of DT_0, DT_5, DT_{10}, and DT_{20}

To further explore the spatial and temporal variation in temperature, we analyzed the trends in DT_0, DT_5, DT_{10}, and DT_{20} over the GLRCA from 1982–2014. At the regional scale, DT_0, DT_5, DT_{10}, and DT_{20} exhibited an overall increasing trend at the rate of 0.437 days/year, 0.485 days/year, 0.451 days/year, and 0.371 days/year, respectively, and all passed the significance test at the 0.01 level (Figure 5). Spatially, the trends in DT_0, DT_5, DT_{10}, DT_{20}, and the uncertainty in the trends were obviously heterogeneous over the entire study area (Figures 6 and 7). The most pronounced increase (>0.6 days/year) in DT_0 was primarily observed in the west and the southeast, accounting for about 29.2% of the study area. Meanwhile, approximately 29.9% of the study area experienced a greater increase (>0.6 days/year) in DT_5, and occurred mainly in the central and southeast. For DT_{10}, the greater increase (>0.6 days/year) was observed mostly in the south, accounting for 19.7% of the study area. About 23.5% of the study area showed a larger increase (>0.6 days/year) in DT_{20}, occurring mainly in the west and south. In addition, a clearly decreasing trend in DT_{20} was observed in the northeast, accounting for approximately 10.8% of the study area. Spatially, the regions with low uncertainty were relatively consistent with those that passed the significance test at the 0.05 level.

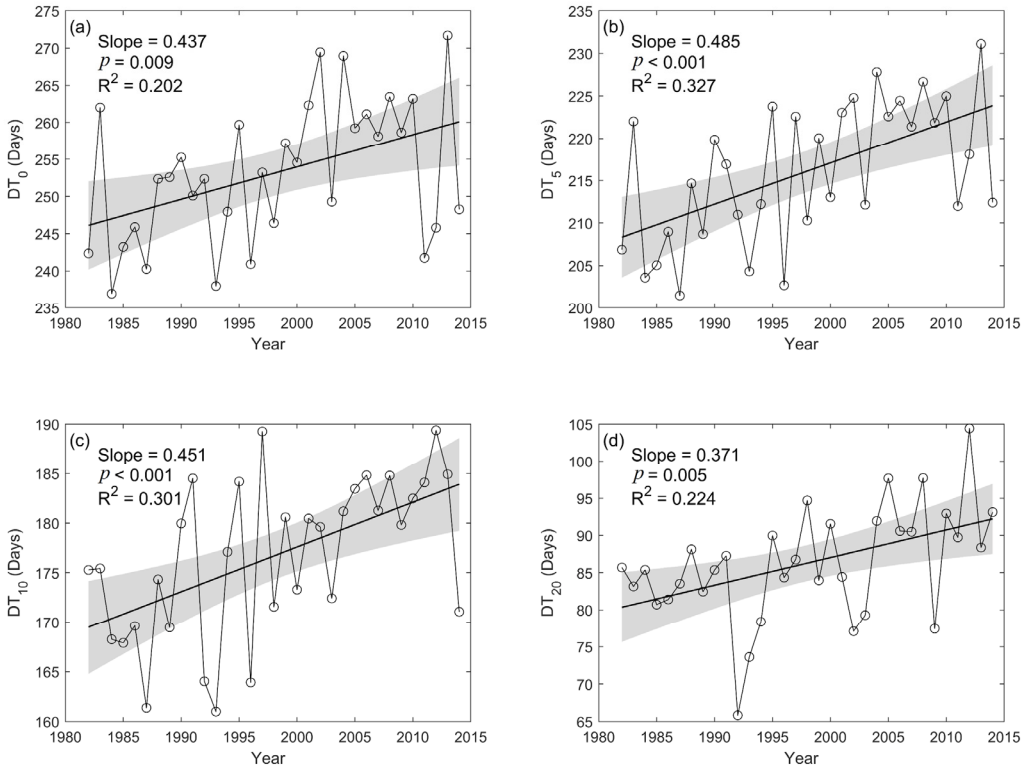

Figure 5. Interannual variations in (**a**) DT_0, (**b**) DT_5, (**c**) DT_{10}, and (**d**) DT_{20} at a regional scale in the GLRCA during the period 1982–2014.

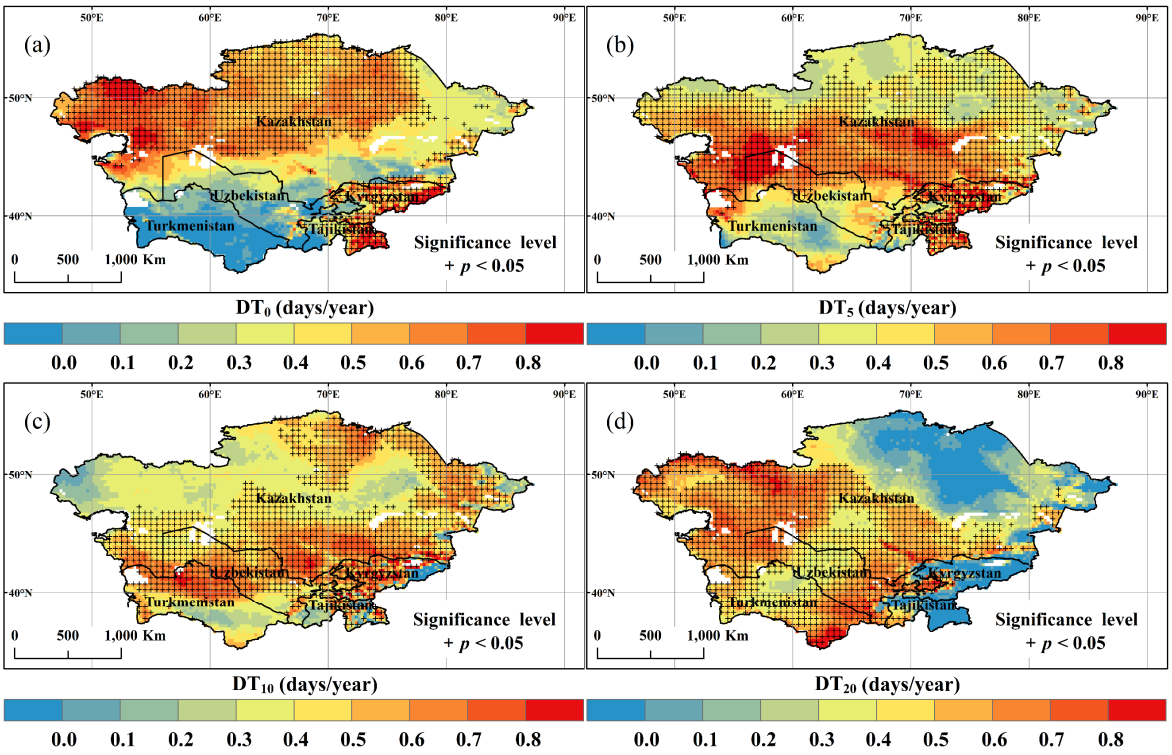

Figure 6. Spatial distribution of trends in (**a**) DT_0, (**b**) DT_5, (**c**) DT_{10}, and (**d**) DT_{20} during the period 1982–2014.

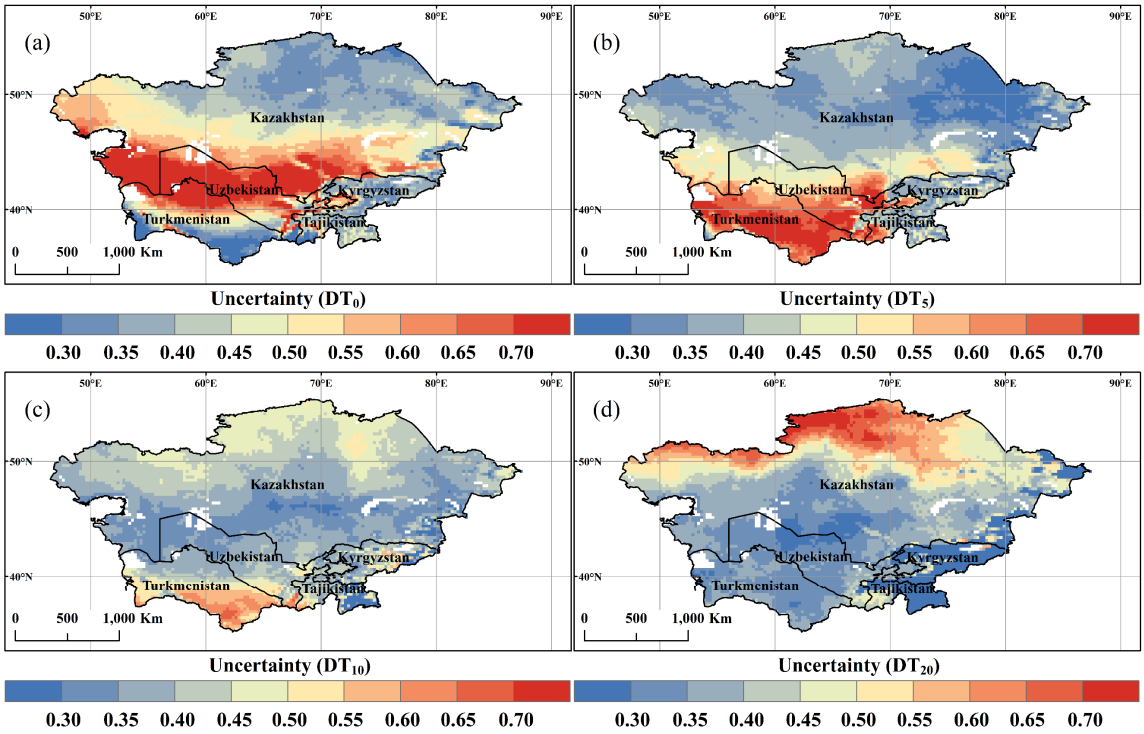

Figure 7. Spatial distribution of uncertainty in the trends of (**a**) DT_0, (**b**) DT_5, (**c**) DT_{10}, and (**d**) DT_{20} during the period 1982–2014.

To further explore the effect of temperature change on vegetation growth, we analyzed the correlation of annual NDVI with DT_0, DT_5, DT_{10}, and DT_{20} across GLRCA for the period 1982–2014 (Figure 8). Spatially, there was a clear heterogeneity in the correlation between the annual NDVI and the four bio-temperature indicators. From 1982 to 2014, positive correlations between annual NDVI with DT_0, DT_5 occurred in 58.8%, 46.6% of the study area, respectively, and greater positive correlations (>0.30) were observed mainly at high elevations in the southeast dominated by cold climate zone. Meanwhile, about 66.6% of the study area was subject to a negative correlation between the annual NDVI and the DT_{10}, especially in the central region with a greater negative correlation (<−0.30). Furthermore, most of the study area (approximately 88.3%) experienced a negative correlation between annual NDVI and DT_{20}, with 43.5% being significant ($p < 0.05$), and the greater negative correlation (<−0.30) was widely distributed in the west. Overall, the larger the number of days with higher temperature, the greater the negative impact on vegetation growth.

3.3. Spatial and Temporal Variation of SGS, EGS, and LGS

Based on daily mean temperature data in the GLRCA from 1982–2014, we further calculated three bio-temperature indicators: SGS, EGS, and LGS. Figure 9 illustrates the interannual trends in SGS, EGS, and LGS at the regional scale in the GLRCA. During the entire study period, SGS exhibited a significant decreasing trend with a regional average rate of −0.261 days/year, and passed the significance test at 0.01 level. Meanwhile, EGS showed a pronounced increasing trend at a rate of 0.164 days/year. Changes in LGS are controlled by changes in SGS and EGS. We further analyzed the interannual trend in LGS and found that LGS across the GLRCA increased at a rate of 0.425 days/year ($p < 0.01$) at the regional scale.

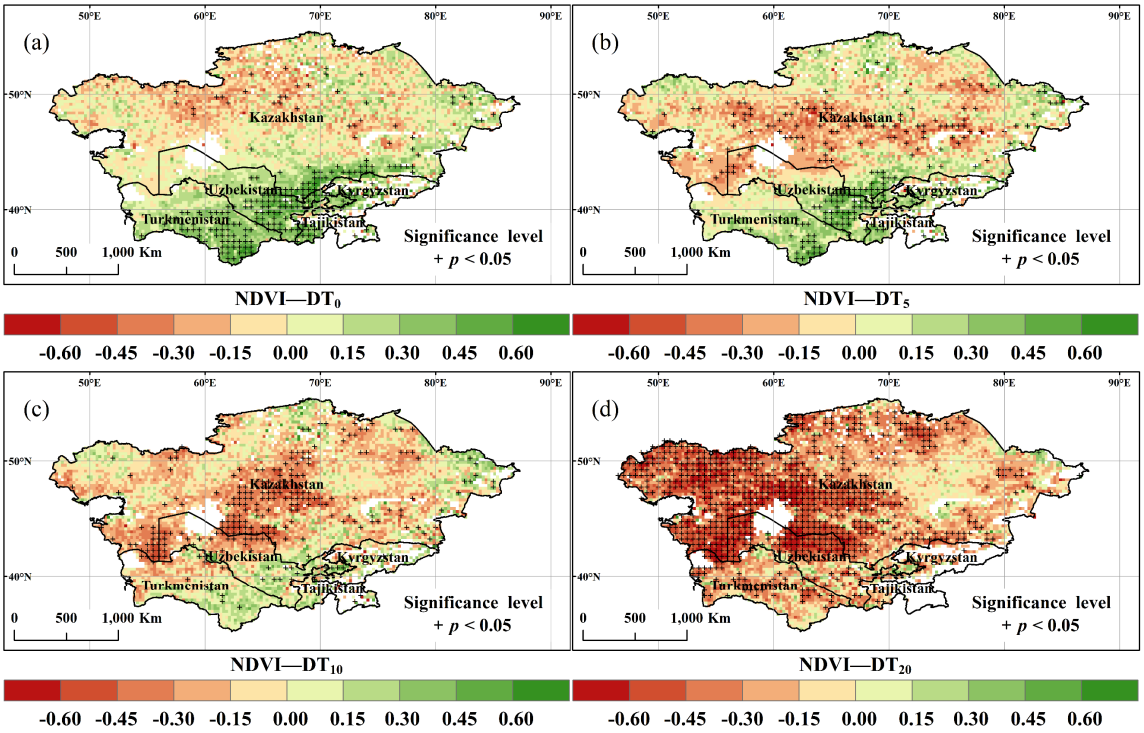

Figure 8. Spatial distribution of correlations between annual NDVI and (**a**) DT_0, (**b**) DT_5, (**c**) DT_{10}, and (**d**) DT_{20} for the period 1982–2014.

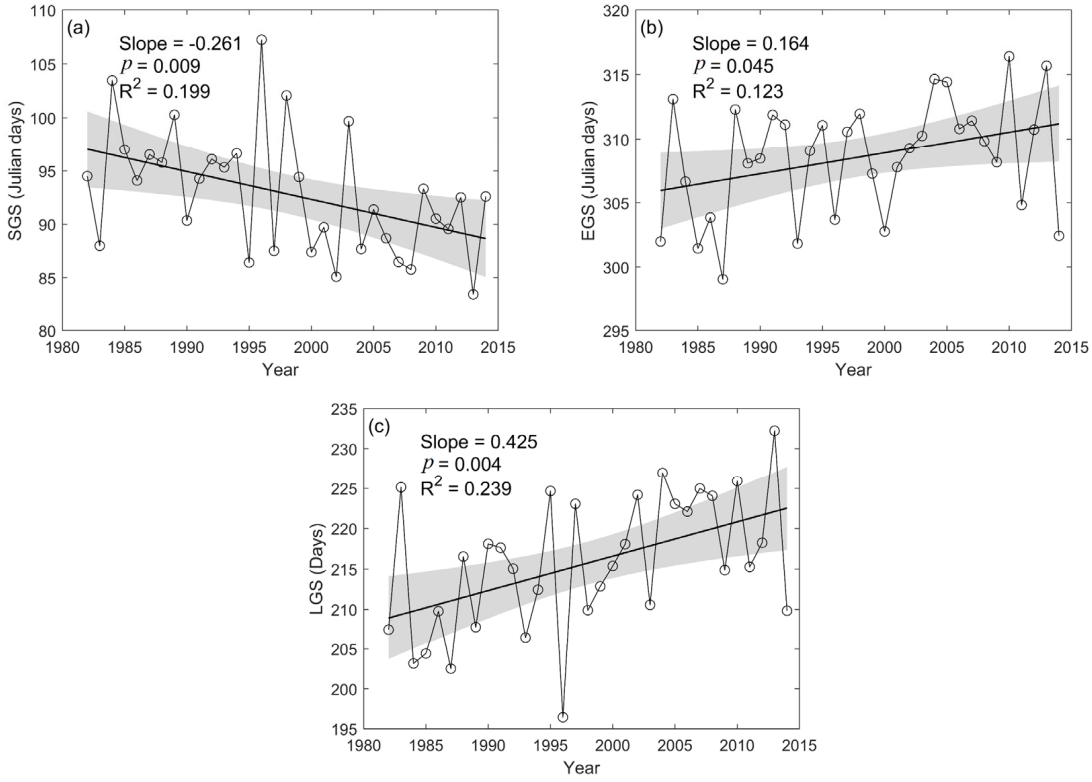

Figure 9. Interannual variations in (**a**) SGS, (**b**) EGS, and (**c**) LGS at a regional scale in the GLRCA during the period 1982–2014.

Figure 10 indicates the spatial distribution of trends in SGS, EGS, and LGS over the GLRCA during the period 1982–2014. Over the past 33 years, most of the study area (about 96.7%) exhibited a negative trend in SGS, with 34.8% being significant ($p < 0.05$). Spatially, the greater advanced SGS (<−0.4 days/year) was mainly observed in the south. For trends in EGS, more than 86.6% of the study area experienced an increasing trend. The larger delays in EGS occurred mainly in the central and southeast. Accompanied by an earlier SGS and a later EGS, LGS showed a pronounced positive trend over 97.8% of the study area, and 34.8% passed the significance test at 0.05 level. Spatially, a higher extended LGS (>0.6 days/year) was observed mainly in the central and southeast. For the uncertainty in the trends of SGS, EGS, and LGS, the low values (<0.35) were mainly in the north, while the high values (>0.65) were mainly in the south (Figure 11).

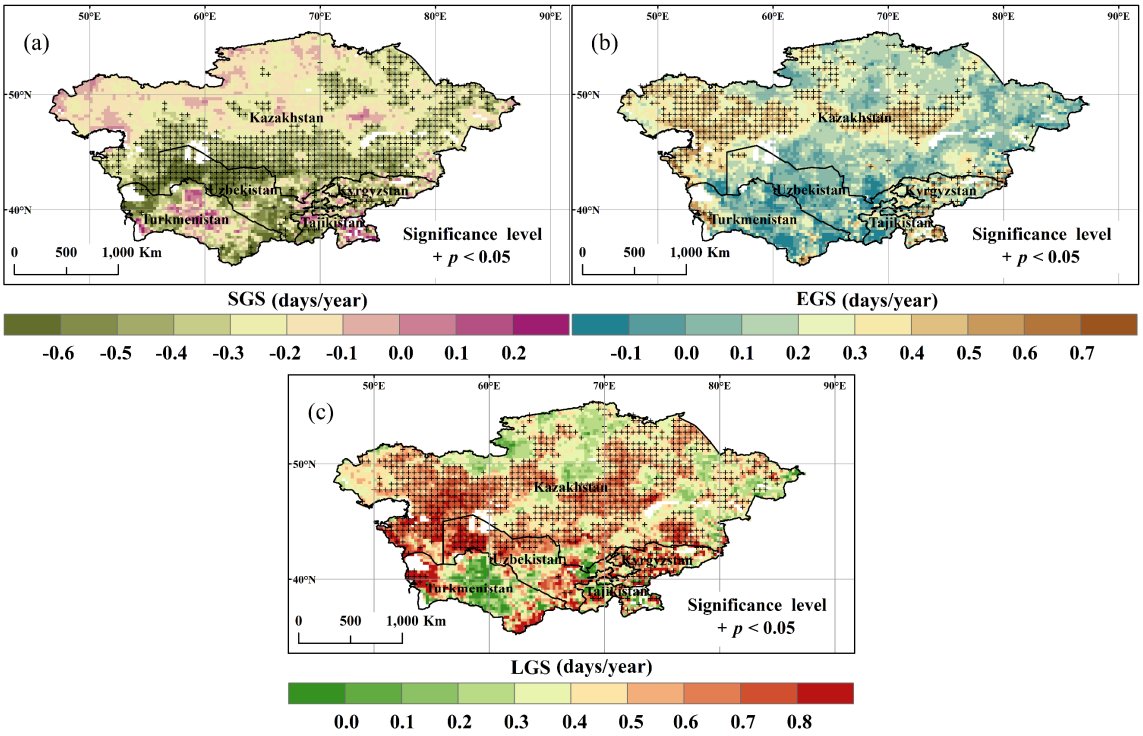

Figure 10. Spatial distribution of trends in (**a**) SGS, (**b**) EGS, and (**c**) LGS for the period 1982–2014.

Temperature is one of the major drivers of vegetation phenology changes. Therefore, we analyzed the correlations between annual NDVI and three indicators of growing season (SGS, EGS, and LGS) derived from surface air temperature to identify the impact of growing season variability on vegetation dynamics (Figure 12). Over the whole study period, the regions showing a positive correlation between annual NDVI and SGS accounted for about 52.2% of the study area. Spatially, the greater positive correlation (>0.2) was occurred mainly in the center of the study area, while the larger negative correlation (<−0.2) was primarily recorded in the north and southeast. Meanwhile, approximately 52.2% of the study area experienced a positive correlation between annual NDVI and EGS, and a larger positive correlation (>0.2) was observed mostly in the south. Then, we analyzed the correlation between annual NDVI and LGS and found that a negative correlation represented approximately 53.6% of the study area. Spatially, the greater negative correlation (<−0.2) between annual NDVI and LGS was mainly found in the central, and the larger positive correlation (>0.2) was mainly in the southeast.

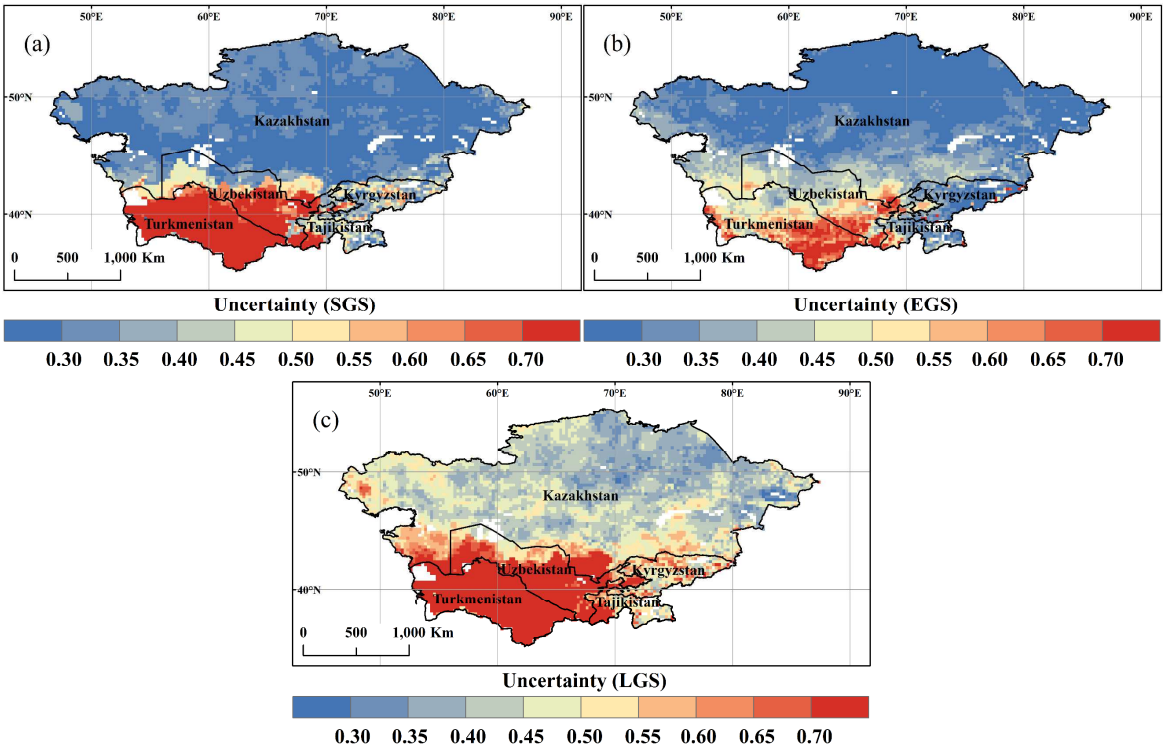

Figure 11. Spatial distribution of uncertainty in the trends of (**a**) SGS, (**b**) EGS, and (**c**) LGS during the period 1982–2014.

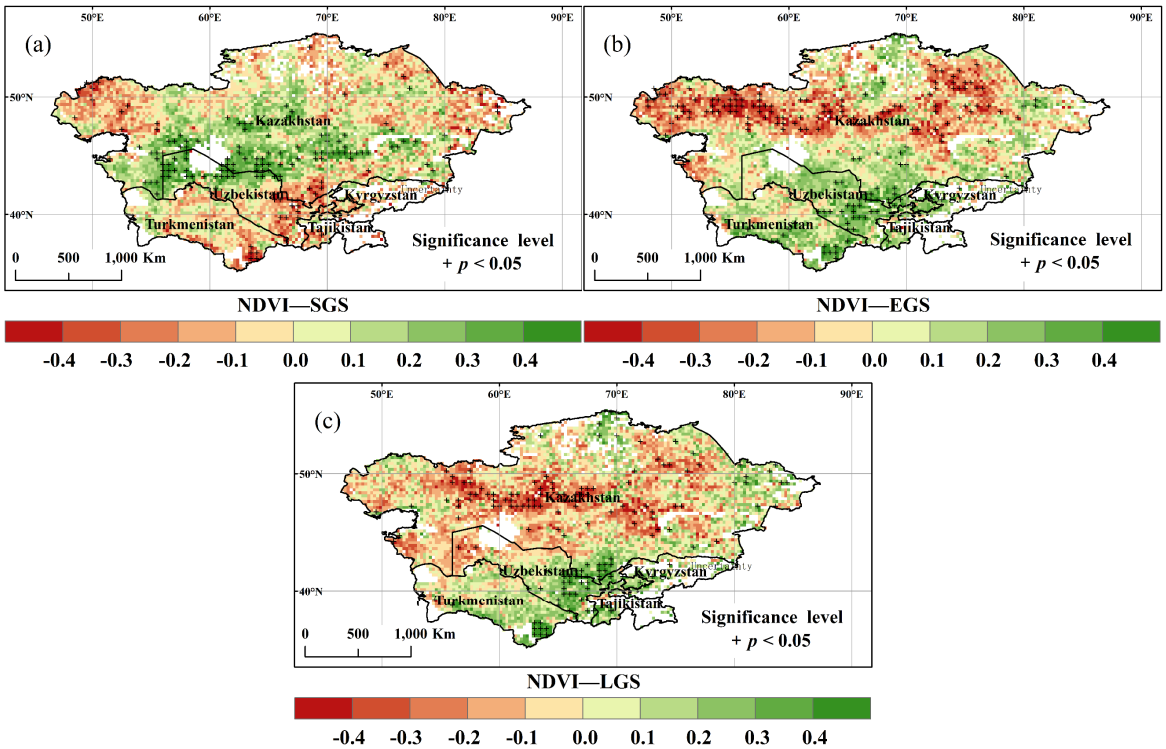

Figure 12. Spatial distribution of correlations between annual NDVI and (**a**) SGS, (**b**) EGS, and (**c**) LGS from 1982–2014.

4. Discussion

In this study, we investigated the spatial and temporal variation of bio-temperature indicators (including DT_0, DT_5, DT_{10}, DT_{20}, SGS, EGS, and LGS), and further analyzed the response of vegetation growth to changes in bio-temperature indicators across the GLRCA for the period 1982–2014.

Over the entire study period, GLRCA experienced a significant warming trend, and such climate warming has induced a series of ecological and environmental effects [59,60]. Since the 1970s, nearly half the great lakes in the GLRCA have shrunk, and considerable glaciers are rapidly retreating due to climate warming [60]. In the present study, a significant decreasing trend in annual NDVI was observed in most of the study area (68.2%), especially around the Aral Sea, while a significant increasing trend was mainly in the east. This variation in vegetation dynamics was also identified in previous studies [19,40]. Meanwhile, numerous studies have suggested that temperature played a major role in the vegetation dynamics across the GLRCA [19,29].

From 1982–2014, approximately 44.0% of the study area experienced a positive correlation between annual temperature and annual NDVI, particularly at high altitudes in the southeast. According to the Koppen–Geiger climate classification [46], GLRCA can be divided into arid climate zone and cold climate zone. Generally, cold climate zones are mainly located at high altitudes, and temperature is the dominant climatic factor affecting vegetation growth [61,62]. Thus, the increase in vegetation greenness in the mountainous of the GLRCA could be attributed to climate warming [19,38]. However, rapid warming could significantly increase evapotranspiration and lead to soil moisture deficit, which in turn limit vegetation growth [63,64]. This might explain the negative correlation of annual NDVI with annual temperature in the west of the study area.

Climate change manifests itself not only as changes in mean conditions, but also as changes in some key bio-temperature thresholds [21]. Key bio-temperature is closely related to the growth of vegetation, and slight changes could produce substantial effects on the structure and function of ecosystems [22,57]. Therefore, we further analyzed the spatial and temporal trends in DT_0, DT_5, DT_{10}, and DT_{20}. Overall, four indicators showed a pronounced increasing trend, which is the consequence of increased temperature in the GLRCA [65]. Spatially, this increase has significant variability, which should be strongly associated with the spatial and temporal heterogeneity in surface characteristics, such as topography and urbanization [66]. Moreover, a clearly decreasing trend in DT_{20} was observed in the northeast, and Figures 3a and 4b revealed that the annual mean temperature in the region also insignificantly increased and the maximum temperature showed a slightly decreasing trend from 1982–2014. Previous studies found that increased precipitation and vegetation greening could induce a cooling effect on regional temperatures [67,68]. Therefore, the increase in precipitation and NDVI over the northeastern GLRCA should contribute to the decrease in DT_{20} [19]. Overall, despite the increasing trend of temperature in the GLRCA, changes in key bio-temperature threshold were variable, and past studies considering only average temperature have limitations.

For the period 1982–2014, the correlations of annual NDVI with DT_0, DT_5, DT_{10}, and DT_{20} were obviously spatially heterogeneous. It implied that the response of vegetation dynamics to temperature drivers was highly variable due to different vegetation characteristics and environmental conditions [29,69]. An increase in DT_0 implies a decrease in frost days. Thus, a slight increase in temperature would exert a positive impact on regional vegetation growth by reducing frost days and extending the growing season [37,70]. At the same time, a significant positive correlation between annual NDVI and temperature indicators was observed at high elevations in the southeast because cold temperature is a serious constraint to vegetation growth in the region [19]. However, most of the regions in GLRCA showed that the negative correlation between DT_0, DT_5, DT_{10}, DT_{20} with annual NDVI increased with increasing bio-temperature thresholds, which may be due to increased temperature intensifying precipitation limitation for dryland vegetation growth [71,72]. In particular, more than 88.3% of the study area showed a negative correlation between

annual NDVI and DT_{20}. In general, DT_{20} occurred mainly in summer, and high temperatures could further increase ecosystem drought. Recently, the negative effects of high temperatures on ecosystems have been widely reported in many regions, especially in arid and semi-arid areas [13,69]. Under high-temperature stress, vegetation photosynthesis is weakened or even stalled, while respiration is enhanced, thus leading to a decrease in productivity [73,74].

Vegetation phenology, including SGS, EGS, and LGS, is a sensitive signal indicating the response of vegetation dynamics to climate change [37,75]. Plenty of remote sensing data and ground observation data demonstrated that spring phenology has advanced and fall phenology has been delayed owing to global warming [24,37,76]. In this study, LGS presented a significant positive trend at a rate 0.425 days/year for the regional scale, and advanced SGS (−0.261 days/year) contributed more relative to delayed EGS (0.164 days/year). This result is consistent with other studies around the globe [37]. Additionally, Li et al. [77] extracted SGS using time series of NDVI, and found that warmer spring temperatures led to advanced SGS, whereas declined spring warming after 2005 reversed the SGS trends. Noticeably, this study also identified two distinct periods around 2005 with opposite SGS trends. In fact, spring cooling has been noted in some regions of the Northern Hemisphere over the last decades [7,78]. Such a spring cooling could possibly result in an insignificant advanced trend of SGS in the north of the study area. Overall, the trends of SGS based on the thermal growing season were relatively consistent with those based on the NDVI time series, which further indicates that the thermal growing season can effectively reflect the response of vegetation growth to temperature change. In addition, the spatial pattern of LGS was similar to that of DT_5 because the growing season in this study was defined based on 5 °C and DT_5 in a year occurred mostly within the growing season.

Environmental changes are inconsistent with the vegetation response, which may lead to different trends in growing season derived from surface air temperature and growing season based on actual vegetation phenology [37,76]. Therefore, we further analyzed the correlations between annual NDVI with SGS, EGS, and LGS. Generally, prolonged LGS controlled by advanced SGS and delayed EGS can increase the time of material accumulation, thereby enhancing vegetation productivity [9,79]. Meanwhile, a pronounced positive correlation between annual NDVI and LGS was observed at high elevations in the southeast. Furthermore, our study found that annual NDVI was negatively correlated with LGS in some regions of the GLRCA, especially in the north. In dryland ecosystems, precipitation is the major driver of vegetation greening, and increased evapotranspiration controlled by climate warming would lead to drought and exacerbate precipitation limitation [80]. In addition, the increase in temperature might accelerate the growth of vegetation and thus lead to a shortening of the vegetation growth cycle, particularly for herbaceous plants [37,81]. Hence, these could explain the negative effect of extended LGS on vegetation growth across the GLRCA.

5. Conclusions

This study analyzed the temporal and spatial characteristics of bio-temperature indicators (DT_0, DT_5, DT_{10}, DT_{20}, SGS, EGS, and LGS) in the GLRCA based on surface air temperature data from 1982–2014, and examined the response of vegetation dynamics to climate change. The major findings are as follows:

(1) With climate warming, DT_0, DT_5, DT_{10}, and DT_{20} all showed a pronounced increasing trend at the regional scale. Spatially, there was significant heterogeneity in the four indicators, particularly an obvious decrease in DT_{20} was observed in the northeast.

(2) Most of the study area showed that the negative correlation between DT_0, DT_5, DT_{10}, DT_{20} with annual NDVI increased with increasing bio-temperature thresholds. In particular, more than 88.3% of the study area experienced a negative correlation between annual NDVI and DT_{20}.

(3) During the entire study period, SGS exhibited a significantly advanced trend at a rate of −0.261 days/year, and EGS experienced a significantly delayed trend at a rate of

0.164 days/year. Therefore, the overall extending trend in LGS was mainly attributed to the advanced SGS.

(4) About 53.6% of the study area showed a negative correlation between annual NDVI and LGS, especially in the north, indicating a negative effect of climate warming on dryland vegetation growth.

Author Contributions: X.G. analyzed the data and wrote the manuscript. D.Z. provided guidance and revised the manuscript. All authors have read and agreed to the published version of the manuscript.

Funding: This study was supported by the Strategic Priority Research Program of the Chinese Academy of Sciences (XDA20020202).

Data Availability Statement: Meteorological data supporting this research are openly available at https://disc.gsfc.nasa.gov/ (accessed on 20 September 2021).

Conflicts of Interest: The authors declare no conflict of interest.

References

1. IPCC. Summary for Policymakers. In *Climate Change 2021: The Physical Science Basis. Contribution of Working Group I to the Sixth Assessment Report of the Intergovernmental Panel on Climate Change*; Masson-Delmotte, V., Zhai, P., Pirani, A., Connors, S.L., Péan, C., Berger, S., Caud, N., Chen, Y., Goldfarb, L., Gomis, M.I., et al., Eds.; Cambridge University Press: Cambridge, UK, 2021.
2. Cheng, W.; Li, Z.; Yan, L. Uniforming spring phenology under non-uniform climate warming across latitude in China. *Sci. Total Environ.* **2021**, *762*, 143177. [CrossRef] [PubMed]
3. Holst, R.; Yu, X.H.; Grun, C. Climate Change, Risk and Grain Yields in China. *J. Integr. Agric.* **2013**, *12*, 1279–1291. [CrossRef]
4. Bolch, T.; Yao, T.; Kang, S.; Buchroithner, M.F.; Scherer, D.; Maussion, F.; Huintjes, E.; Schneider, C. A glacier inventory for the western Nyainqentanglha Range and the Nam Co Basin, Tibet, and glacier changes 1976–2009. *Cryosphere* **2010**, *4*, 419–433. [CrossRef]
5. Zheng, G.H.; Yang, Y.T.; Yang, D.W.; Dafflon, B.; Yi, Y.H.; Zhang, S.L.; Chen, D.L.; Gao, B.; Wang, T.H.; Shi, R.J.; et al. Remote sensing spatiotemporal patterns of frozen soil and the environmental controls over the Tibetan Plateau during 2002–2016. *Remote Sens. Environ.* **2020**, *247*, 19. [CrossRef]
6. Wang, T.H.; Yang, D.W.; Yang, Y.T.; Piao, S.L.; Li, X.; Cheng, G.D.; Fu, B.J. Permafrost thawing puts the frozen carbon at risk over the Tibetan Plateau. *Sci. Adv.* **2020**, *6*, 8. [CrossRef]
7. Wang, X.H.; Piao, S.L.; Ciais, P.; Li, J.S.; Friedlingstein, P.; Koven, C.; Chen, A.P. Spring temperature change and its implication in the change of vegetation growth in North America from 1982 to 2006. *Proc. Natl. Acad. Sci. USA* **2011**, *108*, 1240–1245. [CrossRef]
8. Wei, H.; Zhao, X.; Liang, S.; Zhou, T.; Wu, D.; Tang, B. Effects of Warming Hiatuses on Vegetation Growth in the Northern Hemisphere. *Remote Sens.* **2018**, *10*, 683. [CrossRef]
9. Piao, S.L.; Friedlingstein, P.; Ciais, P.; Viovy, N.; Demarty, J. Growing season extension and its impact on terrestrial carbon cycle in the Northern Hemisphere over the past 2 decades. *Glob. Biogeochem. Cycle.* **2007**, *21*, 11. [CrossRef]
10. Tong, S.Q.; Li, X.Q.; Zhang, J.Q.; Bao, Y.H.; Bao, Y.B.; Na, L.; Si, A.L. Spatial and temporal variability in extreme temperature and precipitation events in Inner Mongolia (China) during 1960–2017. *Sci. Total Environ.* **2019**, *649*, 75–89. [CrossRef]
11. Perkins, S.E.; Alexander, L.V.; Nairn, J.R. Increasing frequency, intensity and duration of observed global heatwaves and warm spells. *Geophys. Res. Lett.* **2012**, *39*, 5. [CrossRef]
12. Liu, Q.; Piao, S.L.; Janssens, I.A.; Fu, Y.S.; Peng, S.S.; Lian, X.; Ciais, P.; Myneni, R.B.; Penuelas, J.; Wang, T. Extension of the growing season increases vegetation exposure to frost. *Nat. Commun.* **2018**, *9*, 426. [CrossRef] [PubMed]
13. Baumbach, L.; Siegmund, J.F.; Mittermeier, M.; Donner, R.V. Impacts of temperature extremes on European vegetation during the growing season. *Biogeosciences* **2017**, *14*, 4891–4903. [CrossRef]
14. Fu, B.; Forsius, M.; Liu, J. Ecosystem services: Climate change and policy impacts Editorial overview. *Curr. Opin. Environ. Sustain.* **2013**, *5*, 1–3. [CrossRef]
15. Ballantyne, A.P.; Alden, C.B.; Miller, J.B.; Tans, P.P.; White, J.W.C. Increase in observed net carbon dioxide uptake by land and oceans during the past 50 years. *Nature* **2012**, *488*, 70–72. [CrossRef]
16. Sitch, S.; Friedlingstein, P.; Gruber, N.; Jones, S.D.; Murray-Tortarolo, G.; Ahlstrom, A.; Doney, S.C.; Graven, H.; Heinze, C.; Huntingford, C.; et al. Recent trends and drivers of regional sources and sinks of carbon dioxide. *Biogeosciences* **2015**, *12*, 653–679. [CrossRef]
17. Yuan, Y.; Bao, A.; Liu, T.; Zheng, G.; Jiang, L.; Guo, H.; Jiang, P.; Yu, T.; De Maeyer, P. Assessing vegetation stability to climate variability in Central Asia. *J. Environ. Manag.* **2021**, *298*, 113330. [CrossRef]
18. Li, H.W.; Li, Y.P.; Huang, G.H.; Sun, J. Quantifying effects of compound dry-hot extremes on vegetation in Xinjiang (China) using a vine-copula conditional probability model. *Agric. For. Meteorol.* **2021**, *311*, 108658. [CrossRef]
19. Jiang, L.L.; Jiapaer, G.; Bao, A.M.; Guo, H.; Ndayisaba, F. Vegetation dynamics and responses to climate change and human activities in Central Asia. *Sci. Total Environ.* **2017**, *599*, 967–980. [CrossRef]

20. Franzke, C.L.E. Local trend disparities of European minimum and maximum temperature extremes. *Geophys. Res. Lett.* **2015**, *42*, 6479–6484. [CrossRef]
21. Zhao, D.S.; Wu, S.H. Spatial and temporal variability of key bio-temperature indicators on the Qinghai-Tibetan Plateau for the period 1961–2013. *Int. J. Climatol.* **2016**, *36*, 2083–2092. [CrossRef]
22. Yang, Y.; Zhao, D.; Chen, H. Variability of bio-climatology indicators in the Southwest China under climate warming during 1961–2015. *Int. J. Biometeorol.* **2019**, *63*, 107–119. [CrossRef]
23. Yin, Y.H.; Deng, H.Y.; Wu, S.H. A new method for generating the thermal growing degree-days and season in China during the last century. *Int. J. Climatol.* **2017**, *37*, 1131–1140. [CrossRef]
24. Dong, M.Y.; Jiang, Y.; Zheng, C.T.; Zhang, D.Y. Trends in the thermal growing season throughout the Tibetan Plateau during 1960–2009. *Agric. For. Meteorol.* **2012**, *166*, 201–206. [CrossRef]
25. Qiu, B.; Lu, Q. A tentative regionalization of agroclimate of China. *Acta Geogr. Sin.* **1980**, *35*, 116–125.
26. Xiao, W.W.; Wang, B.; Liu, D.L.; Feng, P.Y. Projecting Changes in Temperature Extremes in the Han River Basin of China Using Downscaled CMIP5 Multi-Model Ensembles. *Atmosphere* **2020**, *11*, 424. [CrossRef]
27. Xu, L.; Myneni, R.B.; Chapin, F.S.; Callaghan, T.V.; Pinzon, J.E.; Tucker, C.J.; Zhu, Z.; Bi, J.; Ciais, P.; Tommervik, H.; et al. Temperature and vegetation seasonality diminishment over northern lands. *Nat. Clim. Chang.* **2013**, *3*, 581–586. [CrossRef]
28. Piao, S.L.; Wang, X.H.; Ciais, P.; Zhu, B.; Wang, T.; Liu, J. Changes in satellite-derived vegetation growth trend in temperate and boreal Eurasia from 1982 to 2006. *Glob. Chang. Biol.* **2011**, *17*, 3228–3239. [CrossRef]
29. Luo, M.; Sa, C.L.; Meng, F.H.; Duan, Y.C.; Liu, T.; Bao, Y.H. Assessing extreme climatic changes on a monthly scale and their implications for vegetation in Central Asia. *J. Clean Prod.* **2020**, *271*, 122396. [CrossRef]
30. Yao, J.Q.; Chen, Y.N.; Zhao, Y.; Mao, W.Y.; Xu, X.B.; Liu, Y.; Yang, Q. Response of vegetation NDVI to climatic extremes in the arid region of Central Asia: A case study in Xinjiang, China. *Theor. Appl. Climatol.* **2018**, *131*, 1503–1515. [CrossRef]
31. Yao, T.; Chen, F.; Cui, P.; Ma, Y.; Baiqing, X. From Tibetan Plateau to Third Pole and Pan-Third Pole. *Bull. Chin. Acad. Sci.* **2017**, *32*, 924–931. [CrossRef]
32. Li, C.F.; Zhang, C.; Luo, G.P.; Chen, X.; Maisupova, B.; Madaminov, A.A.; Han, Q.F.; Djenbaev, B.M. Carbon stock and its responses to climate change in Central Asia. *Glob. Chang. Biol.* **2015**, *21*, 1951–1967. [CrossRef] [PubMed]
33. Hu, Z.Y.; Zhang, C.; Hu, Q.; Tian, H.Q. Temperature Changes in Central Asia from 1979 to 2011 Based on Multiple Datasets. *J. Clim.* **2014**, *27*, 1143–1167. [CrossRef]
34. Liu, Y.R.; Li, Y.P.; Yang, X.; Huang, G.H.; Li, Y.F. Development of an integrated multivariate trend-frequency analysis method: Spatial-temporal characteristics of climate extremes under global warming for Central Asia. *Environ. Res.* **2021**, *195*, 14. [CrossRef]
35. Zhang, M.; Chen, Y.N.; Shen, Y.J.; Li, B.F. Tracking climate change in Central Asia through temperature and precipitation extremes. *J. Geogr. Sci.* **2019**, *29*, 3–28. [CrossRef]
36. Lioubimtseva, E.; Henebry, G.M. Climate and environmental change in arid Central Asia: Impacts, vulnerability, and adaptations. *J. Arid. Environ.* **2009**, *73*, 963–977. [CrossRef]
37. Wu, L.Z.; Ma, X.F.; Dou, X.; Zhu, J.T.; Zhao, C.Y. Impacts of climate change on vegetation phenology and net primary productivity in arid Central Asia. *Sci. Total Environ.* **2021**, *796*, 15. [CrossRef]
38. Zhou, Y.; Zhang, L.; Fensholt, R.; Wang, K.; Vitkovskaya, I.; Tian, F. Climate Contributions to Vegetation Variations in Central Asian Drylands: Pre- and Post-USSR Collapse. *Remote Sens.* **2015**, *7*, 2449–2470. [CrossRef]
39. Bohovic, R.; Dobrovolny, P.; Klein, D. The Spatial and Temporal Dynamics of Remotely-sensed Vegetation Phenology in Central Asia in the 1982–2011 Period. *Eur. J. Remote Sens.* **2016**, *49*, 279–299. [CrossRef]
40. Zhang, G.L.; Biradar, C.M.; Xiao, X.M.; Dong, J.W.; Zhou, Y.T.; Qin, Y.W.; Zhang, Y.; Liu, F.; Ding, M.J.; Thomas, R.J. Exacerbated grassland degradation and desertification in Central Asia during 2000–2014. *Ecol. Appl.* **2018**, *28*, 442–456. [CrossRef]
41. Trenberth, K.E.; Dai, A.; Rasmussen, R.M.; Parsons, D.B. The changing character of precipitation. *Bull. Am. Meteorol. Soc.* **2003**, *84*, 1205–1217. [CrossRef]
42. Shi, Y.D.; Wang, S.J.; Wang, L.W.; Zhang, M.J.; Argiriou, A.A.; Song, Y.; Lei, S.J. Isotopic evidence in modern precipitation for the westerly meridional movement in Central Asia. *Atmos. Res.* **2021**, *259*, 10. [CrossRef]
43. Bothe, O.; Fraedrich, K.; Zhu, X. Precipitation climate of Central Asia and the large-scale atmospheric circulation. *Theor. Appl. Climatol.* **2012**, *108*, 345–354. [CrossRef]
44. Xu, D.; Li, R.; Wang, C. Characteristics of Precipitation Changes and Relationships with Water Vapor Transport in Typical Arid Regions of Asia and Africa under Global Warming. *Clim. Environ. Res.* **2016**, *21*, 737–748. [CrossRef]
45. Chen, X.; Wang, S.S.; Hu, Z.Y.; Zhou, Q.M.; Hu, Q. Spatiotemporal characteristics of seasonal precipitation and their relationships with ENSO in Central Asia during 1901–2013. *J. Geogr. Sci.* **2018**, *28*, 1341–1368. [CrossRef]
46. Peel, M.C.; Finlayson, B.L.; McMahon, T.A. Updated world map of the Köppen-Geiger climate classification. *Hydrol. Earth Syst. Sci.* **2007**, *11*, 1633–1644. [CrossRef]
47. Goward, S.N. Satellite Bioclimatology. *J. Clim.* **1989**, *2*, 710–720. [CrossRef]
48. Li, Z.; Chen, Y.N.; Li, W.H.; Deng, H.J.; Fang, G.H. Potential impacts of climate change on vegetation dynamics in Central Asia. *J. Geophys. Res. Atmos.* **2015**, *120*, 12345–12356. [CrossRef]
49. Wang, H.L.; Tetzlaff, D.; Buttle, J.; Carey, S.K.; Laudon, H.; McNamara, J.P.; Spence, C.; Soulsby, C. Climate-phenology-hydrology interactions in northern high latitudes: Assessing the value of remote sensing data in catchment ecohydrological studies. *Sci. Total Environ.* **2019**, *656*, 19–28. [CrossRef]

50. Zhong, L.; Su, Z.B.; Ma, Y.M.; Salama, M.S.; Sobrino, J.A. Accelerated Changes of Environmental Conditions on the Tibetan Plateau Caused by Climate Change. *J. Clim.* **2011**, *24*, 6540–6550. [CrossRef]
51. Ji, L.; Senay, G.B.; Verdin, J.P. Evaluation of the Global Land Data Assimilation System (GLDAS) Air Temperature Data Products. *J. Hydrometeorol.* **2015**, *16*, 2463–2480. [CrossRef]
52. Larcher, W.; Biederman-Thorson, M.A. *Physiological Plant Ecology*; Springer: Berlin/Heidelberg, Germany, 1980.
53. Prentice, I.C.; Cramer, W.; Harrison, S.P.; Leemans, R.; Monserud, R.A.; Solomon, A.M. A global biome model based on plant physiology and dominance, soil properties and climate. *J. Biogeogr.* **1992**, *19*, 117–134. [CrossRef]
54. Ruml, M.; Gregoric, E.; Vujadinovic, M.; Radovanovic, S.; Matovic, G.; Vukovic, A.; Pacuca, V.; Stojfcic, D. Observed changes of temperature extremes in Serbia over the period 1961–2010. *Atmos. Res.* **2017**, *183*, 26–41. [CrossRef]
55. Huang, B.W. Draft of the comprehensive physical geographical regionalization of China. *Acta Geogr. Sin.* **1958**, 348–365. [CrossRef]
56. Sillmann, J.; Kharin, V.V.; Zhang, X.; Zwiers, F.W.; Bronaugh, D. Climate extremes indices in the CMIP5 multimodel ensemble: Part 1. Model evaluation in the present climate. *J. Geophys. Res. Atmos.* **2013**, *118*, 1716–1733. [CrossRef]
57. Yin, Y.H.; Deng, H.Y.; Wu, S.H. Spatial-temporal variations in the thermal growing degree-days and season under climate warming in China during 1960–2011. *Int. J. Biometeorol.* **2019**, *63*, 649–658. [CrossRef]
58. Cornes, R.C.; van der Schrier, G.; Squintu, A.A. A reappraisal of the thermal growing season length across Europe. *Int. J. Climatol.* **2019**, *39*, 1787–1795. [CrossRef]
59. Liu, H.J.; Chen, Y.N.; Ye, Z.X.; Li, Y.P.; Zhang, Q.F. Recent Lake Area Changes in Central Asia. *Sci Rep.* **2019**, *9*, 11. [CrossRef]
60. Yu, Y.; Chen, X.; Malik, I.; Wistuba, M.; Cao, Y.G.; Hou, D.D.; Ta, Z.J.; He, J.; Zhang, L.Y.; Yu, R.D.; et al. Spatiotemporal changes in water, land use, and ecosystem services in Central Asia considering climate changes and human activities. *J. Arid Land.* **2021**, *13*, 881–890. [CrossRef]
61. Wang, Q.X.; Fan, X.H.; Wang, M.B. Recent warming amplification over high elevation regions across the globe. *Clim. Dyn.* **2014**, *43*, 87–101. [CrossRef]
62. Wang, Z.Q.; Cui, G.L.; Liu, X.; Zheng, K.; Lu, Z.Y.; Li, H.L.; Wang, G.N.; An, Z.F. Greening of the Qinghai-Tibet Plateau and Its Response to Climate Variations along Elevation Gradients. *Remote Sens.* **2021**, *13*, 3712. [CrossRef]
63. Anderegg, W.R.L.; Kane, J.M.; Anderegg, L.D.L. Consequences of widespread tree Mortality triggered by drought and temperature stress. *Nat. Clim. Chang.* **2013**, *3*, 30–36. [CrossRef]
64. Zhang, W.; Li, Y.; Wu, X.; Chen, Y.; Chen, A.; Schwalm, C.R.; Kimball, J.S. Divergent Response of Vegetation Growth to Soil Water Availability in Dry and Wet Periods Over Central Asia. *J. Geophys. Res. Biogeosci.* **2021**, *126*, e2020JG005912. [CrossRef]
65. Feng, R.; Yu, R.D.; Zheng, H.W.; Gan, M. Spatial and temporal variations in extreme temperature in Central Asia. *Int. J. Climatol.* **2018**, *38*, E388–E400. [CrossRef]
66. Toelle, M.H.; Churiulin, E. Sensitivity of Convection-Permitting Regional Climate Simulations to Changes in Land Cover Input Data: Role of Land Surface Characteristics for Temperature and Climate Extremes. *Front. Earth Sci.* **2021**, *9*, 722244. [CrossRef]
67. Yuan, X.; Wang, W.; Cui, J.; Meng, F.; Kurban, A.; Maeyer, P.D. Vegetation changes and land surface feedbacks drive shifts in local temperatures over Central Asia. *Sci. Rep.* **2017**, *7*, 3287. [CrossRef]
68. Barbero, R.; Westra, S.; Lenderink, G.; Fowler, H.J. Temperature-extreme precipitation scaling: A two-way causality? *Int. J. Climatol.* **2018**, *38*, E1274–E1279. [CrossRef]
69. Li, S.; Wei, F.L.; Wang, Z.; Shen, J.S.; Liang, Z.; Wang, H.; Li, S.C. Spatial Heterogeneity and Complexity of the Impact of Extreme Climate on Vegetation in China. *Sustainability* **2021**, *13*, 5748. [CrossRef]
70. Zhao, D.; Gao, X.; Yang, Y. Trends of freezing period and its main cause on the Qinghai-Tibetan Plateau from 1961 to 2018. *Theor. Appl. Climatol.* **2021**, *146*, 1355–1366. [CrossRef]
71. Zhang, C.; Lu, D.S.; Chen, X.; Zhang, Y.M.; Maisupova, B.; Tao, Y. The spatiotemporal patterns of vegetation coverage and biomass of the temperate deserts in Central Asia and their relationships with climate controls. *Remote Sens. Environ.* **2016**, *175*, 271–281. [CrossRef]
72. Wu, X.C.; Guo, W.C.; Liu, H.Y.; Li, X.Y.; Peng, C.H.; Allen, C.D.; Zhang, C.C.; Wang, P.; Pei, T.; Ma, Y.J.; et al. Exposures to temperature beyond threshold disproportionately reduce vegetation growth in the northern hemisphere. *Natl. Sci. Rev.* **2019**, *6*, 786–795. [CrossRef]
73. von Buttlar, J.; Zscheischler, J.; Rammig, A.; Sippel, S.; Reichstein, M.; Knohl, A.; Jung, M.; Menzer, O.; Arain, M.A.; Buchmann, N.; et al. Impacts of droughts and extreme-temperature events on gross primary production and ecosystem respiration: A systematic assessment across ecosystems and climate zones. *Biogeosciences* **2018**, *15*, 1293–1318. [CrossRef]
74. Salvucci, M.E.; Crafts-Brandner, S.J. Inhibition of photosynthesis by heat stress: The activation state of Rubisco as a limiting factor in photosynthesis. *Physiol. Plant.* **2004**, *120*, 179–186. [CrossRef] [PubMed]
75. Richardson, A.D.; Anderson, R.S.; Arain, M.A.; Barr, A.G.; Bohrer, G.; Chen, G.S.; Chen, J.M.; Ciais, P.; Davis, K.J.; Desai, A.R.; et al. Terrestrial biosphere models need better representation of vegetation phenology: Results from the North American Carbon Program Site Synthesis. *Glob. Chang. Biol.* **2012**, *18*, 566–584. [CrossRef]
76. Sun, Q.L.; Li, B.L.; Zhou, G.Y.; Jiang, Y.H.; Yuan, Y.C. Delayed autumn leaf senescence date prolongs the growing season length of herbaceous plants on the Qinghai-Tibetan Plateau. *Agric. For. Meteorol.* **2020**, *284*, 11. [CrossRef]
77. Li, C.; Wang, R.; Cui, X.; Wu, F.; Yan, Y.; Peng, Q.; Qian, Z.; Xu, Y. Responses of vegetation spring phenology to climatic factors in Xinjiang, China. *Ecol. Indic.* **2021**, *124*, 107286. [CrossRef]

78. Sun, C.; Kucharski, F.; Li, J.P.; Wang, K.C.; Kang, I.S.; Lian, T.; Liu, T.; Ding, R.Q.; Xie, F. Spring Aleutian Low Weakening and Surface Cooling Trend in Northwest North America During Recent Decades. *J. Geophys. Res. Atmos.* **2019**, *124*, 12078–12092. [CrossRef]
79. Richardson, A.D.; Black, T.A.; Ciais, P.; Delbart, N.; Friedl, M.A.; Gobron, N.; Hollinger, D.Y.; Kutsch, W.L.; Longdoz, B.; Luyssaert, S.; et al. Influence of spring and autumn phenological transitions on forest ecosystem productivity. *Philos. Trans. R. Soc. B Biol. Sci.* **2010**, *365*, 3227–3246. [CrossRef]
80. Ma, X.L.; Huete, A.; Moran, S.; Ponce-Campos, G.; Eamus, D. Abrupt shifts in phenology and vegetation productivity under climate extremes. *J. Geophys. Res. Biogeosci.* **2015**, *120*, 2036–2052. [CrossRef]
81. Sherry, R.A.; Zhou, X.H.; Gu, S.L.; Arnone, J.A.; Schimel, D.S.; Verburg, P.S.; Wallace, L.L.; Luo, Y.Q. Divergence of reproductive phenology under climate warming. *Proc. Natl. Acad. Sci. USA* **2007**, *104*, 198–202. [CrossRef]